www.czasopisma.pan.pl PAN www.journals.pan.pl
POLSKA AKADEMIA NAUK

ARCHIVE OF MECHANICAL ENGINEERING

DOI: 10.24425/ame.2026.157611 2026, Vol. 73, No. 1, pp. 125–147

Fethi DJAAD[1], Brahim MEBARKI[2], Djallel ZEBBAR[1], Sahraoui KHERRIS[1], Momen S.M. SALEH[3]

Numerical investigation of a new fin configuration in a PCM-filled triplex tube heat exchanger incorporating nanoparticles

Received 1 August 2025, **Revised** 29 December 2025, **Accepted** 4 January 2026, **Published online** 12 March 2026

Keywords: triplex tube, PCM RT82, nanofluids, new fin, thermal storage

This study evaluates the thermal performance of phase change material (PCM) in a triplex tube heat exchanger (TTHE) integrated with flat-plate solar collectors. To enhance the PCM melting rate, the heat exchanger system incorporates newly designed fin geometries and nanoparticle additives. A numerical parametric analysis was conducted to evaluate the effects of fin dimensions (length and thickness) in conjunction with average temperature, liquid fraction, and various nanofluids (Al_2O_3, CuO, and TiO_2). Model validation was performed by comparing the predicted temperature distribution with previously published numerical and experimental data, thereby confirming the model's reliability. The results indicate that adding Al_2O_3 nanoparticles improves the melting rate by 31.6%, while the optimized fin geometry enhances heat distribution and reduces the melting time by 32.5% compared to conventional configurations. These findings contribute to the development of more efficient latent heat thermal energy storage systems (LTES). Additionally, preliminary integration of a circulation system and learning mechanism is proposed as a promising approach for future performance enhancement.

✉ Sahraoui KHERRIS, e-mail: kherris.sahraoui@univ-tissemsilt.dz

[1] Laboratory of Mechanical Engineering, Materials and Structures, Department of Civil, Mechanical, and Transportation Engineering, Tissemsilt University, Tissemsilt, Algeria

[2] Laboratory of Mechanics, Modeling and Experimentation. Department of Mechanical Engineering, University of Bechar Tahri Mohamed, Bechar, Algeria

[3] Laboratory of Materials and Energy Engineering, University of Mohamed Khider, Biskra, Algeria

Nomenclature

C	Constant reflection of the mushy zone
H	Enthalpy (J)
h	Sensible enthalpy ($J\cdot kg^{-1}$)
g	Gravity acceleration ($m\cdot s^{-2}$)
k	Thermal conductivity ($W\cdot m^{-1}\cdot K^{-1}$)
p	Pressure ($N\cdot m^{-2}$)
T	Temperature (K)
c_p	Specific heat ($J\cdot kg^{-1}\cdot K^{-1}$)
u_i	Kinematic viscosity
H_{ref}	Reference enthalpy ($J\cdot kg^{-1}$)
T_{ref}	Reference temperature (K)
ΔH	Latent heat content between (solid) and (liquid)

Greek letters

ρ	Density ($kg\cdot m^{-3}$)
μ	Dynamic viscosity ($kg\cdot m^{-1}\cdot s^{-1}$)
β	Thermal expansion coefficient (K^{-1})
γ	Liquid fraction
$\emptyset$	Nanoparticle concentration

Subscripts

s	Solid
l	Liquid
ref	Reference
HTF	Heat transfer fluid
TES	Thermal energy storage
PCM	Phase change material
PCMs	Phase change materials
NEPCM	Nanoparticle enhanced PCM
LTES	Latent thermal energy storage

1. Introduction

Energy plays a crucial role in global development. However, the growing dependence on fossil fuels and their unsustainable consumption pose a serious threat to the energy security of many countries. In response to this challenge, it is essential to explore sustainable alternatives to ensure a reliable and environmentally friendly energy supply. Among these alternatives, solar energy emerges as a promising solution, despite its inherent limitations, particularly its intermittency and limited storage capacity. To overcome these challenges, researchers and energy storage specialists are actively developing innovative solutions to improve the efficiency and reliability of storage systems.

These innovative approaches are being actively studied to enhance the efficiency and reliability of energy storage systems. Notably, sensible heat storage, which involves accumulating heat in a material by increasing its temperature; latent heat storage, which leverages phase change materials (PCMs) to store and release energy; and thermochemical storage, which utilizes reversible chemical reactions to store and release heat more efficiently [1].

Among various approaches employed in latent thermal energy storage (LTES), the use of phase change materials is a key focus of research. Their ability to store large amounts of energy at nearly constant temperatures during phase transitions makes them particularly attractive for advanced thermal storage applications [2].

To accelerate heat transfer in latent thermal energy storage systems, various techniques have been employed, including the use of extended fins [3], porous metals [4, 5], and nanomaterials [6, 7].

The most commonly encountered storage system integrates a heat exchanger containing a PCM. Two types of heat exchangers are generally used: triplex heat exchangers and coaxial heat exchangers [8]. To increase the heat exchange surface area and thereby enhance heat transfer performance and system efficiency, the integration of fins has been widely adopted in previous studies [8–16].

For instance, Mat et al. [9] demonstrated that adding straight fins, both internally and externally, to a triplex tube heat exchanger reduced the melting time of PCM RT82 by 43.3%. Maintaining the same configuration, Al-Abidi et al. [10] studied several parameters, including flow rate, temperature, and HTF circulation, by replacing axial flow with radial flow. They found that temperature and flow rate inversely affected the PCM melting time and that a radial inlet helped reduce this melting time. In line with the study by Arsalan Yawar et al. [11], a detailed analysis was conducted on a triplex tube heat exchanger under three operational modes: charging-only, simultaneous charging/discharging, and discharging-only. It was found that the horizontal configuration with charging through the outer tube and discharging through the inner tube was the most effective, reducing charging time by 41%.

In addition, Al-Abidi et al. [8] demonstrated that the effect of varying the configuration of the tube through the number and placement of fins is important in improving the melting process. The results also showed that the eight-cell PCM architecture achieves shorter melting times, resulting in a 34.7% reduction in overall melting time.

With a different fin geometry, Yan et al. [12] demonstrated that using Y-shaped fins in triplex tubes improves heat transfer efficiency by optimizing thermal contact between the PCM and heat exchange surfaces.

In a similar vein, triplex tubes with V-shaped fins were found to be more effective than nanoparticles at accelerating PCM solidification by Alizadeh et al. [13].

Furthermore, Chih-Che Chueh et al. [14] numerically studied the melting process of a phase change material and the use of a triplex tube with H-shaped fins in a concentric shell-and-tube configuration. Properly arranged H-shaped fin structures are considered a preferable design, as they can either enhance heat transfer or increase the latent storage energy.

In addition, Ben Palmer et al. [15] investigated the design and optimization of a W-shaped fin configuration informed by flow dynamics for a triplex tube, aiming to accelerate the PCM melting process and enable faster energy storage rates. The results showed that the optimized fin geometry could achieve a 57.4% reduction in melting time. It was found that curved fins performed better than similar straight fins.

Also, Hassan Waqas et al. [16] demonstrated in the present study that integrating triangular fins with multistage inner tubes in a triplex-tube configuration plays a crucial role in enhancing the melting process of PCM. The results revealed that optimized configurations can significantly reduce melting time, highlighting the effectiveness of geometric design and nanoparticle additives in overcoming the low thermal conductivity of paraffin wax.

Similarly, Aman Kumar et al. [17] designed a rotational storage unit configuration with traditional straight fins. The melted fraction, temperature distribution, and velocity variation were analyzed to assess the thermal performance and fluid flow dynamics. They demonstrated that a higher rotational speed led to a higher rate of PCM discharge. The discharge was faster in the straight-fin unit than in the wave-shaped fin unit when there was no rotation or when the rotational speed was low.

Moreover, tree-shaped fin structures were designed by Zeinab Esmaeili et al. [18] to identify the optimal fin shape that provides the greatest thermal energy in a heat exchanger containing PCM RT82. They compared the new designs with a conventional structure during the melting and solidification processes. The new design demonstrated a reduction in melting and solidification times by 7.36% and 23.70%, respectively, compared to the conventional design.

In a study conducted by Mohamed Boujelbene et al. [19], arch-shaped fins were employed in a horizontal triplex-tube thermal storage system to investigate the effects of fin design on melting performance. The optimized fin configuration resulted in a reduction of melting time by up to 53% and a significant enhancement in heat storage capacity compared to finless configurations.

Another interesting approach was proposed by Ren et al. [20], who investigated snowflake fins in a triplex tube for PCM melting and solidification, achieving better heat distribution and a particularly significant improvement in heat exchangers, particularly in triple tube designs. They also demonstrated the importance of fins in increasing the surface area available for heat transfer and improving heat transfer performance and overall system efficiency.

Beyond fin configurations, one practical and innovative solution in the field of latent heat storage is the use of PCMs, which can store and release large amounts of thermal energy through phase transitions. Upon absorbing heat, they transform from a solid to a liquid state, and upon releasing heat, they return to their solid state, which allows them to store and release thermal energy as needed [21]. PCMs are utilized in various applications, including thermal energy storage systems [22], heating and cooling in buildings [23], air conditioning, enhancing the efficiency of solar cells, and maintaining the appropriate temperatures for preserving medicines and food [24]. PCMs are also used to transport goods in refrigerated vehicles [25] and to maintain safe temperature ranges for electronic devices. Due to their high energy storage capacity, PCMs contribute to improving the energy efficiency and reducing the environmental impact of heating and cooling systems. In this regard, M. Javidan et al. [3] conducted a comprehensive thermal evaluation to investigate the effect of wall transparency on the melting process in paraffinic materials and the role of heat radiation. Their results showed that increasing the heat flux significantly amplifies the effects of heat transfer. Additionally, by incorporating radiation effects, the melting process of paraffin materials was enhanced by 31%.

To further enhance PCM performance, incorporating nanoparticles into PCMs increases the thermal conductivity of PCMs, leading to more efficient TES. Scientific contributions in this field include understanding the behavior of PCM and considering the influence of different types of nanoparticles on improving the performance of PCMs.

For instance, Ji Zhang et al. [26] incorporated novel substructured fibers and aluminum oxide nanoparticles to improve the performance of PCMs during the solidification process in a triplex tube heat exchanger. The application of the nanoparticles and metal fibers significantly improved the solidification behavior. A reduction in solidification time by 8.5%, 9.3%, and 10.3% was observed for aluminum oxide nanoparticles (2%, 5%, and 8%, respectively).

Along the same lines, Soroush Entezari et al. [27] enhanced the melting performance of PCMs in an innovative (TES) unit that combines triplex-tube and helical-coil configurations. To accelerate the melting process, the study examined the impact of incorporating TiO_2, Al_2O_3, and CuO nanoparticles into pure PCM at various volume fractions. The most significant improvement was observed with Al_2O_3 at a 4% volume fraction, resulting in a 13.3% reduction in melting time compared to pure PCM.

A study by Burcu Çiçek [28] presented a numerical analysis showing that the addition of nanoparticles such as Fe_3O_4, MgO, ZnO, and xGNP to the phase change material RT35HC significantly improved the heat sink performance. The melting time was reduced by up to 14.56%, with Fe_3O_4 at a 0.02 volume fraction achieving the lowest base temperature.

Similar to the work of Prashant Saini et al. [29], Cesaro fin configurations were investigated to enhance PCM melting under various conditions. Their study demonstrated that natural convection enhanced the melting rate by 26.8%, and optimized fin designs improved temperature uniformity and heat transfer. Furthermore, combining copper metal foam with nanoparticles (Cu, CuO, Al_2O_3) led to a 63.4% reduction in melting time due to improved thermal conductivity and synergistic effects.

Another study conducted by Saleh Al Arni et al. [30] numerically investigated an LTES system using zigzag-shaped tubes combined with Al_2O_3 nanoparticles. They found that the solidification time was reduced by 75% compared to straight tubes with pure PCM, highlighting the effectiveness of both geometric modifications and nanoparticle enhancements in improving discharge performance.

This numerical investigation explores the thermal behavior of a phase change material in a triplex tube heat exchanger (TTHE) coupled with flat-plate solar collectors. The study emphasizes the improvement of heat transfer efficiency during the melting phase through the application of advanced engineering techniques. Specifically, optimizing the fin geometry enables a higher fin density, resulting in a more uniform and efficient thermal distribution within the exchanger.

To this end, the model was tested to investigate the effect of innovative fin designs in the triplex tube on optimizing heat flow distribution. Furthermore, the study assessed the impact of incorporating nanoparticles (Al_2O_3, CuO, TiO_2) to enhance thermal conductivity of the PCM and accelerate its phase transition. The study relies on a detailed numerical model to evaluate the influence of the fins' geometric parameters (length and thickness), as well as analyzing the effects of average temperature and liquid fraction ratio within the PCM. Furthermore, the accuracy of the developed mathematical model is validated through comparisons with published numerical and experimental data, reinforcing its reliability and effectiveness in optimizing TES systems and supporting the development of more efficient and sustainable thermal energy technologies. Based on previous research, a preliminary integration of circulation systems and learning mechanisms is proposed as a promising approach for future performance enhancement.

2. System description

The solar energy unit is a fully integrated system developed to harness solar energy for thermal power generation (Fig. 1). The unit comprises three main components: a flat-plate solar collector, which absorbs sunlight and converts it into

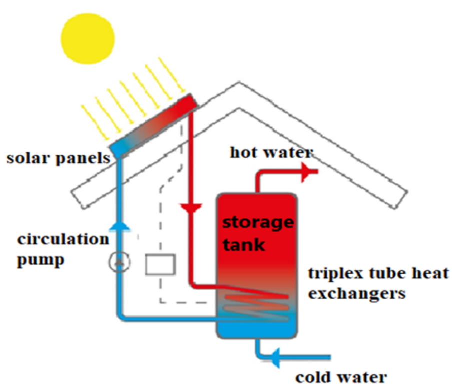

Fig. 1. The solar energy unit

thermal energy through a heat transfer fluid (HTF); a pump, which circulates the fluid to ensure efficient heat transfer between the collector and the storage unit; and a storage unit consisting of a triplex tube heat exchanger that utilizes latent thermal energy for later use, particularly during nighttime or in the absence of solar radiation. The storage unit utilizes PCMs for TES, ensuring continuity and sustainability of thermal energy supply for various applications.

3. Numerical simulations

3.1. Geometry configuration

The adopted geometry, featuring a triplex unit, incorporates an innovative design aimed at enhancing thermal energy storage efficiency. The system consists of three concentric tube layers embedded within one another, which enhance the heat transfer process to and from the thermal energy storage material (see Fig. 2a). This triplex tube configuration not only increases the heat transfer surface area but also improves the rate of energy exchange during charging and discharging cycles. In this setup, phase change material RT82 is filled in the annular region between the inner and outer tubes, as illustrated in Fig. 2a. The triplex tube design increases the surface area available for heat exchange, thereby enhancing the melting and solidification rates of the PCM. The geometric dimensions of the triplex tube heat exchanger are presented in Table 1 [8]. To further improve thermal performance, longitudinal fins are attached to the inner and outer tube walls and are fully immersed in the PCM, as illustrated in Fig. 2b. In addition to the fin-based enhancements, melting performance will be further improved by incorporating

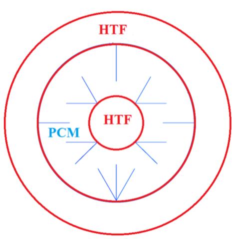

(a) Physical domain

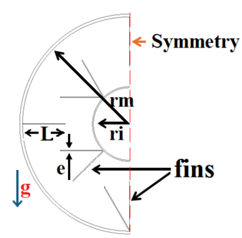

(b) Computational domain

Fig. 2. Configuration model triplex tube

Table 1. Sizing of a triplex tube

Tube	Inter radius (mm)	Outer radius (mm)	Thickness (mm)
Inner	25.4	26.6	1.2
Intermediate	75	77	2
Outer	98	100	2

various types of nanoparticles into the PCM. Simultaneously, the geometric parameters of the fins, such as their length and thickness, will be optimized to enhance overall thermal efficiency.

The thermophysical properties of the three types of PCM, RT82, RT50, and RT60, are presented in Table 2, providing crucial information such as melting points, latent heat, and thermal conductivity, which are essential for understanding their behavior in the heat exchanger system.

Table 2. Comparative thermophysical data for PCM and copper materials

Property	RT50	RT60	RT82	Copper
Density (solid) ($kg\,m^{-3}$)	880	880	950	8978
Density (liquid) ($kg\,m^{-3}$)	760	770	770	–
Specific heat ($J{\cdot}kg^{-1}{\cdot}K^{-1}$)	2000	2000	2000	381
Fusion's latent heat ($J\,kg^{-1}$)	168	160	176	–
Conductivity ($W{\cdot}m^{-1}{\cdot}K^{-1}$)	0.2	0.2	0.2	387.6
Coefficient of thermal expansion (K^{-1})	0.0006	0.0005	0.001	–
Viscosity dynamics ($kg{\cdot}m^{-1}{\cdot}s^{-1}$)	0.0048	0.0288	0.03499	–

Following this, the study examines various geometrical configurations for fins used in heat exchangers. The detailed geometric parameters of these fins, including their thickness (Th) and length (L), as well as the operational fluid temperature for heat transfer, are specified in Table 3. These parameters are critical, as they directly impact the system's heat transfer efficiency and overall performance. By investigating various configurations, the study aims to optimize the design for enhanced thermal management and improved effectiveness in heat exchanger applications.

Table 3. Numerical simulation cases

Case	Length (mm)		Thickness (mm)	T_{HTF} (K)
	Inner	Outer		
Case A	30	30	0.5	363
Case B	35	35	0.5	363
Case C	40	40	0.5	363
Case D	45	45	0.5	363

3.2. Grid sensitivity and time step size

Grid sensitivity analysis involves adjusting the grid resolution to assess how changes in grid size affect simulation results (see Fig. 3). This analysis is crucial for determining the optimal grid resolution that strikes a balance between com-

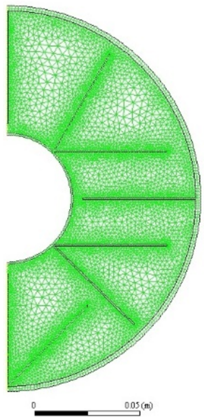

Fig. 3. The model of grid distribution

putational efficiency and the accuracy of the results. The present study evaluated various grid resolutions, including 11 799, 13 000, and 17 630, as shown in Fig. 4. The analysis revealed that a grid resolution of 17 692 provides the most reliable representation of the system while maintaining computational efficiency and avoiding distortions caused by overly coarse or excellent grids.

Time step size analysis examines how variations in time step size impact the accuracy and stability of the simulation. Time steps that are too large can lead to numerical inaccuracies and instability, while time steps that are too small can result in excessive computational costs. The study compares three sets of element numbers (as shown in Fig. 5) to assess the impact of different time step sizes (0.3, 0.5, and 1 seconds) on the simulation outcomes. Through time step size analysis, the appropriate time step size of 0.3 s is determined to provide a reliable representation of transient phenomena while maintaining computational efficiency.

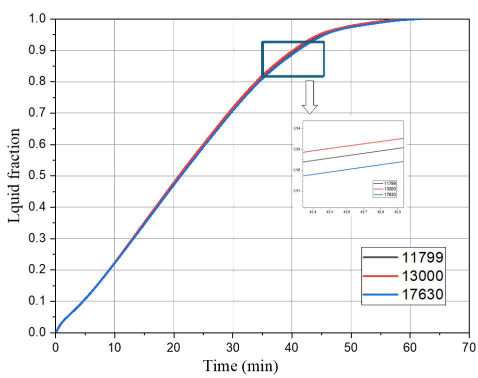

Fig. 4. Comparison of liquid fractions for different grid sizes

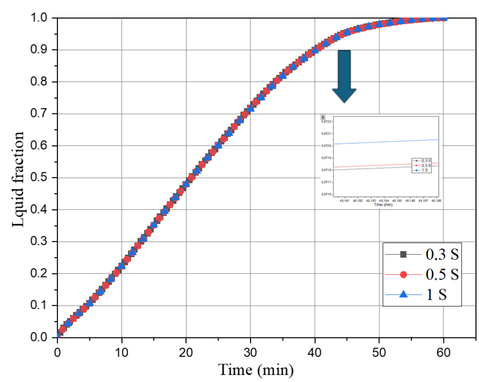

Fig. 5. Comparison of liquid fractions for different time step sizes

3.3. Boundary conditions

The melting process is initiated with the PCM entirely in its solid state, with an initial temperature of 300 K. The tube wall, which serves as the temperature (HTF) interface, is maintained at a constant temperature of 363 K. The boundary conditions applied to the heat exchanger (triplex tube), as well as the internal fins, were systematically varied to analyze their effects on the thermal performance and melting dynamics of the PCM. These boundary conditions can be specified as follows:

The boundary conditions adopted for the interior:

$$r = r_i \quad \rightarrow \quad T = T_{\mathrm{HTF}}\,, \tag{1}$$

$$r = rm \quad \rightarrow \quad \partial T/\partial r = 0. \tag{2}$$

The boundary conditions adopted for the exterior:

$$r = r_i \quad \rightarrow \quad \partial T/\partial r = 0, \tag{3}$$

$$r = rm \quad \rightarrow \quad T = T_{\mathrm{HTF}}\,. \tag{4}$$

Heating both sides method:

$$r = r_i \quad \rightarrow \quad T = T_{\mathrm{HTF}}\,, \tag{5}$$

$$r = rm \quad \rightarrow \quad T = T_{\mathrm{HTF}}\,. \tag{6}$$

Initial temperature for all models:

$$t = 0 \quad \rightarrow \quad T = T_{\mathrm{inital}}\,. \tag{7}$$

3.4. Governing equation

The model used for simulating the melting of phase change materials RT82 incorporates a laminar, incompressible flow and a transient physical model to describe the dynamic behavior of the phase change process. This model is built on the fundamental principles of conservation: mass, momentum, and energy. It assumes that viscous dissipation is negligible, simplifying the analysis by excluding the effects of viscosity. The analysis considers the constant thermophysical properties of the PCM, as listed in Table 2, including viscosity, thermal conductivity, and specific heat. The effect of natural convection during the melting process is accounted for using the Boussinesq approximation, which is applicable when variations in buoyancy force density are present. Outside of this condition, buoyancy effects are neglected.

The density variation is formally defined as [31]:

$$\begin{aligned} \rho &= \rho_m \left[1 - \beta\left(T - T_m\right)\right], \\ \rho_m &= \left(\rho_s + \rho_l\right)/2. \end{aligned} \tag{8}$$

The equations utilized for this situation are continuity, momentum, and energy ones expressed as [32]:

Continuity:

$$\partial_t(\rho) + \partial_i(\rho u_i) = 0. \tag{9}$$

Momentum:

$$\partial_t(\rho u_i) + \partial_j\left(\rho u_i u_j\right) = \mu\partial_{jj}u_i - \partial_i p + \rho g_i + S_i\,, \tag{10}$$

where S_i, the source term for the porosity function defined by Brent et al. [33], is defined as:

$$S_i = C(1-\gamma)^2\frac{u_i}{\gamma^3+\varepsilon}\,. \tag{11}$$

The equations used in this study are analogous to Carman-Kozeny equations for the flow in porous media. In this context, the constant C represents the characteristic morphology of the mushy zone. For this study, a value of $C = 10^5$ was used [34]. Additionally, $\varepsilon = 0.001$ is employed to avoid division by zero issues.

Energy:

$$\partial_t(\rho h) + \partial_t(\rho\Delta H) + \partial_i(\rho u_i h) = \partial_i(k\partial_i T). \tag{12}$$

The bellow equation defines enthalpy H as:

$$H = h + \Delta H\,, \tag{13}$$

where sensible enthalpy h is defined as:

$$h = h_{\mathrm{ref}} + \int\limits_{T_{\mathrm{ref}}}^{T} c_p\,\mathrm{d}T. \tag{14}$$

The liquid fraction of the PCM, γ, is generated during the phase change between the solid and liquid states when the temperature is between $T_l > T > T_s$, and can be expressed as:

$$\gamma = \begin{cases} 0 & \text{if } T < T_s\,, \\ 1 & \text{if } T > T_l\,, \\ \dfrac{(T-T_s)}{(T_l-T_s)} & \text{if } T_l > T > T_s\,. \end{cases} \tag{15}$$

Boussinesq approximation was adopted to calculate the change in PCM density as a function of temperature in the liquid density given by:

$$\rho = \rho_0\left[1-\beta\,(T-T_0)\right]. \tag{16}$$

The corresponding relationship for buoyancy forces in the momentum equation is given by:

$$-\rho g = \rho_0 g\left[\beta\,(T-T_m)-1\right], \tag{17}$$

where ρ_0 is the reference density at melting temperature T_m and β is the thermal expansion.

The density of NEPCM can be computed as:

$$\rho_{\text{NEPCM}} = \rho_{\text{PCM}} \left[(1 - \emptyset) + \emptyset \left(\frac{\rho_s}{\rho_{\text{PCM}}} \right) \right], \tag{18}$$

where $\emptyset$ is the volume fraction of nanoparticles.

The subscripts np, n, and p stand for NEPCM, nanoparticles, and PCM, respectively.

The heat capacity of the NEPCM is expressed as:

$$\rho c_{p\text{NEPCM}} = \rho c_{p\text{PCM}} \left[(1 - \emptyset) + \emptyset \left(\frac{\rho C p_s}{\rho C p_{\text{PCM}}} \right) \right]. \tag{19}$$

Based on the expressions presented in [35], the effective dynamic viscosity of the NEPCM is calculated as follows:

$$\mu_{\text{NEPCM}} = \frac{\mu_{\text{PCM}}}{(1 - \emptyset)^{2.5}}. \tag{20}$$

The effective thermal conductivity of NEPCM can be computed using the Hamilton-Crosser model based on the Maxwell theory [36]:

$$k_{\text{NEPCM}} = \frac{k_s + (S-1)k_{\text{PCM}} - (S-1)\emptyset\,(k_{PCM} - k_s)}{k_s + (S-1)k_{\text{PCM}} + \emptyset\,(k_{\text{PCM}} - k_s)} k_{\text{PCM}}, \tag{21}$$

where S is the particle shape factor.

3.5. Selection of nanofluids

To effectively utilize nanoparticles in thermal systems, it is essential to select the particles based on specific criteria, including high thermal conductivity, excellent stability, low density, and cost-effectiveness. In this study, three types of nanoparticles were selected: aluminum oxide (Al_2O_3), copper oxide (CuO), and titanium oxide (TiO_2). The correlations of Khanafer et al. determine the thermophysical properties of nanofluids [37]. The physical properties of the nanoparticles (CuO, Al_2O_3, and TiO_2) are provided in Table 4.

3.6. Numerical modeling

The storage model with the new fin configuration has been developed, and the validation conditions are maintained using ANSYS FLUENT simulation software in two dimensions. The SIMPLE algorithm is employed for pressure-velocity coupling, and the PRESTO scheme. The scheme is used for solving the pressure correction equation. A second-order scheme is applied for momentum and energy

Table 4. Thermophysical properties of nanofluids

Property	Nanoparticle (AL_2O_3)	Nanoparticle (CuO)	Nanoparticle (TiO_2)
Cp (J·kg^{-1}·K^{-1})	765	535.6	686.2
ρ (kg·m^{-3})	3970	5600	4250
k (W·m^{-1}·K^{-1})	40	20	8.9538
β (K^{-1})	0.85×10^{-5}	1.74×10^{-5}	0.9×10^{-5}

corrections. Furthermore, to solve the mass, momentum, and energy equations, the QUICK approach was used.

Furthermore, the numerical solution was stabilized by carefully calibrating the solution controls. Under-relaxation factors were set to 0.3 for pressure, 0.2 for momentum, 0.9 for the liquid fraction update, and 1.0 for energy to ensure convergence and accuracy. These settings were chosen to ensure numerical stability and to facilitate convergence during the iterative solution process. Convergence criteria are achieved at each time step with a maximum of 150 iterations, ensuring the reliability of the current numerical approach for further computations.

4. Result and discussion

4.1. Result validation

This study builds upon the experimental and numerical work of Sohif et al. [9], using the same physical model. Numerical simulations were carried out on a triplex tube heat exchanger under identical thermophysical conditions. The validity of the developed model was verified by comparing the results for average temperature with those reported by Sohif et al. The model had already been validated in previous research [8], and the strong agreement between the two sets of results is confirmed, as illustrated in Fig. 6.

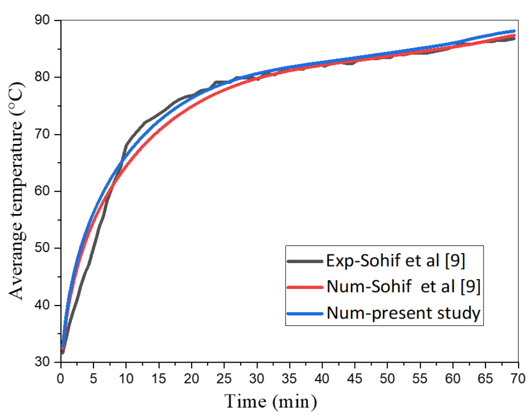

Fig. 6. Validation with experimental and numerical results compared by [9]

4.2. CFD simulation with the new fin's configuration

The present study focuses on enhancing the melting of PCM in triplex tube heat exchangers by adding fins, in addition to optimizing the geometric parameters of the selected fin, including length, width, and thickness. The reading of the simulation results is provided from temperature and liquid fraction contours. To investigate the effects of HTF and different types of PCM, the simulation results are graphically presented and discussed.

4.2.1. Effect of fin length on the melting process

Fig. 7 illustrates the effect of fin lengths (L) on the liquid fraction and average temperature distribution. With a fixed (HTF) of a (T = 363 K), the fin lengths investigated are 30, 35, 40, and 45 mm. The curve of case D, with a length of 45 mm, presents the shortest melting time, at 32.5 minutes, compared to the other cases. Additionally, the average temperature reached its maximum value for this case, resulting in an accelerated melting process. The fin length has a significant impact on the melting time. The increased heating and accelerated melting in case D were due to the increased heat exchange area, which resulted in better heat distribution. Therefore, a 45-mm-long new fin is the most appropriate length for the present study.

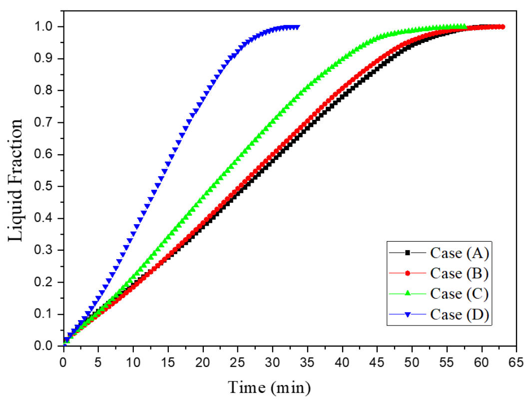

Fig. 7. Effect of the length on the melting PCM

4.2.2. Contours of length fin improvement of heat transfer

This section presents the effect of fin length on the liquid fraction melting of PCM in the heat exchanger (triplex tube). With the heating internal-external method of Sohif et al. [9], the fin's lengths of (30, 35, 40, and 45) and contours showed different melting times (15, 30, 45 and 60 min) as illustrated in (Fig. 8), it can be observed that, initially, the liquid fraction appeared on both the internal and

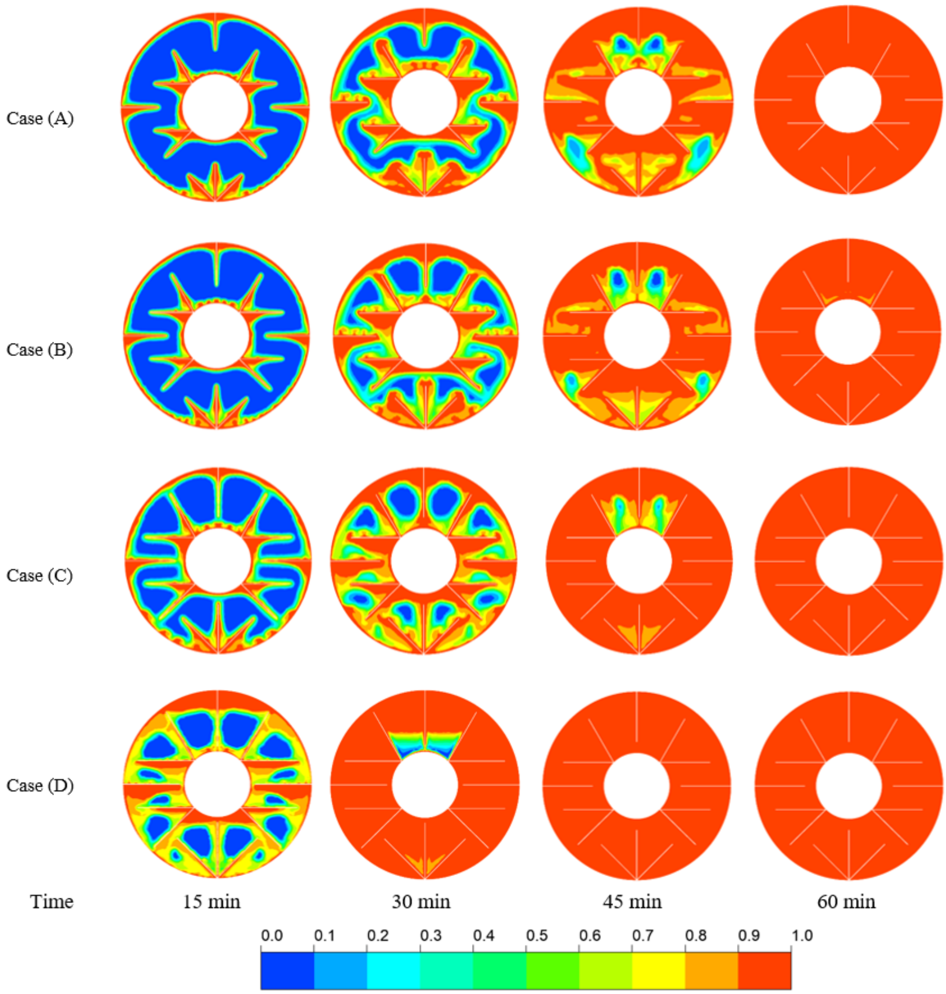

Fig. 8. A liquid fraction contours with variation of length over time

external surfaces of the tube, including the fins. Additionally, there were discernible mean circulations present in the lower portion of the tube. It can be observed that as the mixing time passes, the volume of the fluid increases due to improvements in heat transfer by conduction and convection. After 45 minutes, the fluid begins to expand upward, reflecting the effect of convection on the melting process. After that, the annular spaces become almost entirely covered by fluid after 60 minutes. It can also be observed that there is a variation in the melting rates, which is due to the locations of the fins and their effective role in enhancing heat exchange. The aforementioned results demonstrated that the 45 mm fin provided the best performance and heat exchange, as it enhanced heat transfer by increasing the effective area and reducing thermal resistance, resulting in the shortest melting time compared to the studied lengths, as shown in Table 5.

Table 5. Melting time with different fin lengths

CASE	A	B	C	D
Length (mm)	30	35	40	45
Melting time (min)	62.5	61.5	57.5	32

Fig. 9 illustrates how the heat flux is distributed within the studied system under the influence of various operational factors, such as the actual fin length (L = 30, 35, 40, 45 mm) and the time available for heat exchange. The fins play a crucial role in enhancing heat transfer through both convection and conduction mechanisms. Initially, the heat distribution appears uniform due to similar initial

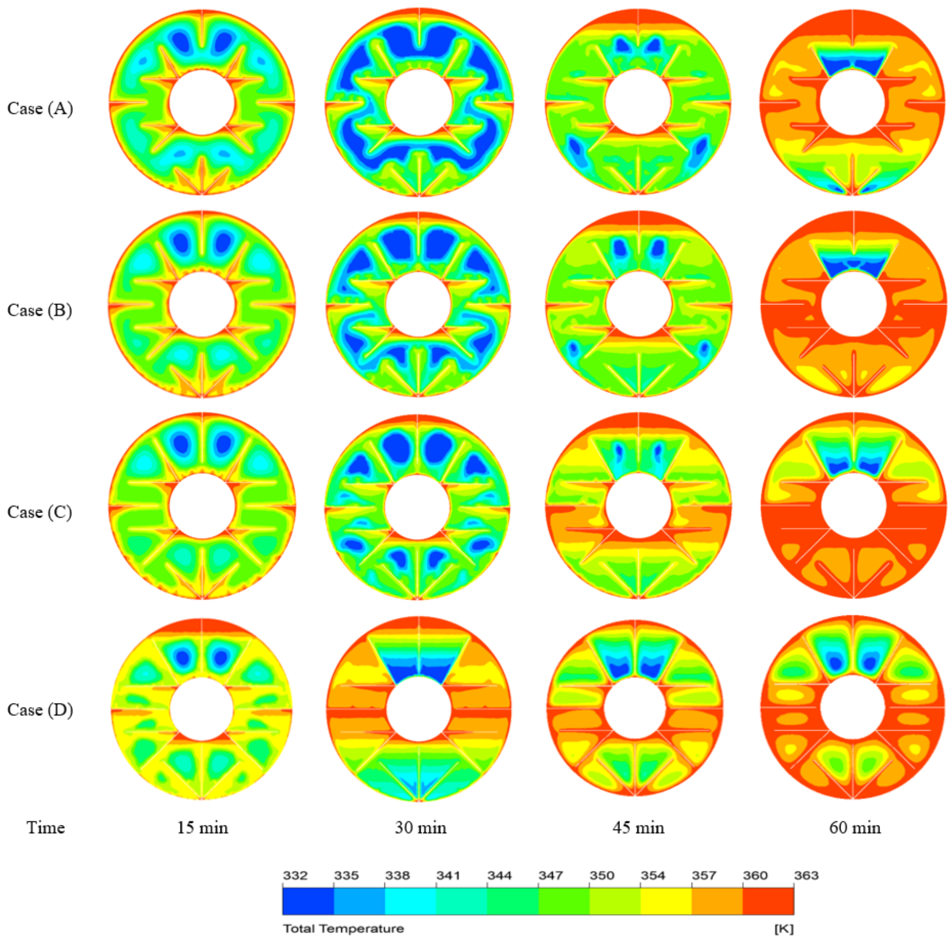

Fig. 9. Average temperature contours with variation of length over time

heating conditions. Over time, the temperature in the areas near the fins gradually rises due to direct heat transfer to them. The effect of the fins in enhancing heat transfer to the (PCM) can be observed, as slight temperature differences appear between the areas near the fins and those farther from them.

In addition, natural convection plays a significant role over time. The density of the substance varies between the liquid and solid stages, causing this to happen. The heated fluid can rise inside the system because its density is lower than that of the solid. When compared to shorter fin lengths, this impact improves the system's average temperature, increases the PCM melting rate, and reduces thermal differences by allowing heat to circulate more evenly in all directions. Conversely, when fins are shorter (30 mm), the effect of heat transfer is limited to the media near the surfaces, resulting in more pronounced thermal gradients within the PCM. These gradients increase thermal resistance, slowing the melting process and resulting in a less uniform heat distribution.

Thus, fin length is a crucial factor in enhancing the thermal performance of the system. Longer fin lengths (45 mm) outperform shorter ones by reducing thermal resistance and achieving a more uniform temperature distribution, thereby enhancing heat transfer efficiency and the system's thermal response.

4.2.3. The effect of new fin thickness on the liquid fraction

Fig. 10 illustrates the relationship between fin thickness and the melting time of the phase change material (PCM) for fin thicknesses of 0.5 mm, 1 mm, and 2 mm, while maintaining a constant fin length and an operating temperature of 363 K. The results indicate a slight reduction in melting time with increasing fin thickness. This behavior can be attributed primarily to the enhancement of conductive heat transfer within thicker fins, which facilitates more effective heat delivery to the PCM.

Despite this improvement, the overall influence of fin thickness on the melting process remains limited, as evidenced by the relatively small differences in melt-

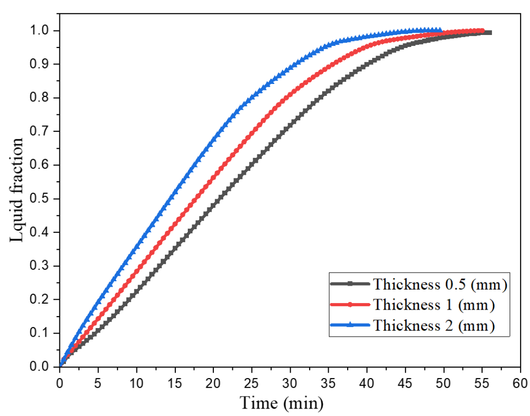

Fig. 10. Effect of fin thickness on the melting phase change material

ing times, which are approximately 56, 55, and 50 minutes for fin thicknesses of 0.5 mm, 1 mm, and 2 mm, respectively. These findings suggest that fin thickness has a comparatively minor effect on the PCM melting behavior under the investigated operating conditions. Consequently, the use of thinner fins can be considered a favorable design choice, as it enables a larger volume of PCM to be accommodated within the heat exchanger, thereby increasing the thermal energy storage capacity and improving material utilization efficiency without significantly degrading the thermal performance of the system.

4.2.4. The effect of temperature (HTF) on the liquid fraction

Fig. 11 depicts the influence of the heat transfer fluid (HTF) temperature on the melting duration of a phase change material PCM at three distinct temperatures: 363 K, 368 K, and 373 K, using the optimized configuration. The findings indicate that the melting duration at a HTF temperature of 363 K is 53.5 minutes, decreasing to 38 minutes at 368 K, and further to 32 minutes at 373 K.

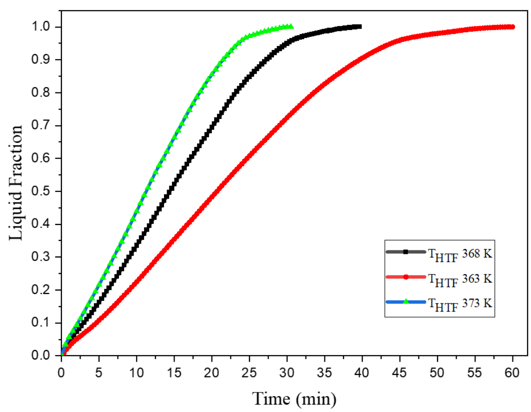

Fig. 11. Variation of PCM's liquid melting fraction according to heat transfer fluid temperature

The figure shows an inverse relationship between melting time and temperature. Increasing thermal conductivity with increasing temperature enhances the transfer of thermal energy to the phase change material, resulting in a more efficient melting process.

Therefore, it can be concluded that the best and preferred choice for applications requiring rapid heat transfer is to select a higher temperature, given its role in enhancing the efficiency of the melting process, as higher temperatures significantly contribute to reducing the melting time.

4.2.5. The effect of PCM type on melting time

Fig. 12 shows the effect of different types of phase change materials RT82 on the melting time at a heat exchanger temperature (HTF) of 363 K. The types studied are RT82, RT60, and RT50. According to the data, RT82 has the greatest melting time (32.5 minutes), followed by RT60 (19.5 minutes) and RT50 (16.5 minutes). The melting time, which depends on the particular melting temperature of each kind of PCM, explains these variations. Because of increased thermal energy transfer efficiency, the melting time decreases as the melting temperature approaches the HTF temperature.

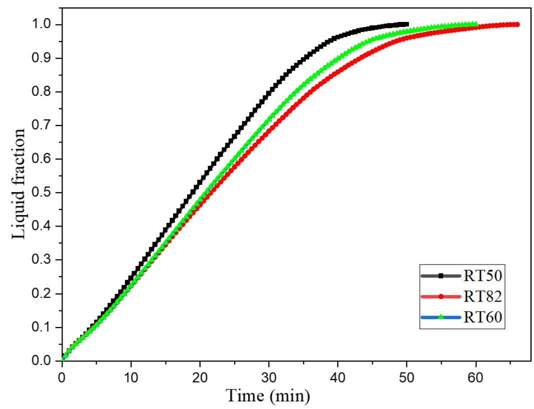

Fig. 12. Variation of the liquid melting fraction according to the phase change material type

On the other hand, the system takes longer to finish the melting process when the melting temperature is greater than the HTF temperature. Consequently, it appears that the thermal storage goal determines which PCM type is most suitable. Short melting times are more effectively achieved by materials whose melting temperatures are closer to the working temperature. Higher-temperature storage, such as RT82, is more effective in terms of thermal capacity and is thus a better option for applications that require more energy storage.

4.3. CFD simulation with PCM incorporating nanoparticles

Incorporating nanoparticles into phase change materials (PCM) influences the coalescence behavior during melting, thereby enhancing their thermal conductivity and heat transfer characteristics. This section investigates the effect of three different nanoparticles: aluminum oxide (Al_2O_3), copper oxide (CuO), and titanium dioxide (TiO_2), each introduced at a constant concentration of 3% in the pure PCM.

4.3.1. The effect of nonadditive incorporation

Fig. 13 presents the variation in the liquid fraction of three nano-enhanced phase change materials (nano-PCMs), each incorporating a uniform nanoparticle volume fraction of 3%, compared to pure PCM during the melting (charging) process. The nanoparticles selected for this study include aluminum oxide (Al_2O_3), copper oxide (CuO), and titanium dioxide (TiO_2). The melting curves indicate a notable decrease in the melting time upon the incorporation of nanoparticles into the PCM. The pure PCM exhibited the longest melting time, reaching 3600 seconds, reflecting its limited thermal conductivity. In contrast, the addition of Al_2O_3, CuO, and TiO_2 nanoparticles significantly enhanced the heat transfer process, resulting in reduced melting durations of 2550 s, 2520 s, and 2580 s, respectively. Among the tested nanoparticles, Al_2O_3 nanoparticles are cost-effective and widely available in uniform sizes, providing significant thermal enhancement. This improvement is mainly attributed to their high thermal conductivity and more stable dispersion within the PCM compared to other nanoparticles.The accelerated melting process and improved heat transfer efficiency observed with Al_2O_3 clearly underscore its effectiveness in enhancing the thermal behavior of PCM-based thermal management systems during the charging phase.

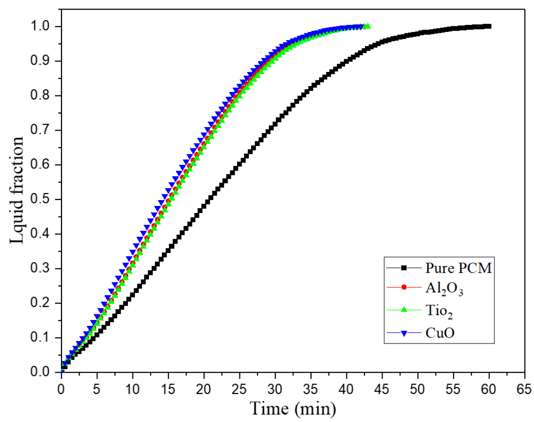

Fig. 13. Variation of the liquid melting fraction according to the nanoparticles type

5. Conclusion

The thermal analysis of the melting process of a phase change material for thermal energy storage in a three-tube heat exchanger was investigated. A novel approach was employed to enhance the fin contact surface, incorporating nanofluids into the phase change material RT82 storage module. Simulations were performed using ANSYS Fluent software to evaluate the performance and efficiency of the TES module proposed in this study. The phase change behavior during thermal charging, as well as in the presence and absence of various nanoparticles, was also investigated. The results showed the following:

- The integration of the new fin designs reduced the melting time by 31%.
- The new fins showed better improvement due to improved temperature distribution.

- The fin design is simple and increases the contact surface between the fins and the PCMs.
- This design also increased the volume of the PCM to 1050 mm^3, allowing for greater energy storage capacity.
- The incorporation of nanoparticles (Al_2O_3, CuO, and TiO_2) into the phase change material (PCM) at a 3% volume fraction resulted in a significant enhancement of heat transfer performance and a notable reduction in melting time. Among the nanoparticles evaluated, aluminum oxide (Al_2O_3) demonstrated the most significant improvement, decreasing the melting time from 3600 seconds for pure PCM to 2550 seconds.

These findings confirm that the combined effects of enhanced fin design and nanoparticle addition in a triplex tube heat exchanger can significantly improve the thermal performance of latent heat thermal energy storage systems. The reduction in melting time, improvement in temperature distribution, and increased PCM volume all contribute to faster charging rates and higher energy storage density. The proposed design significantly improved thermal energy storage performance.

References

[1] G. Li. Sensible heat thermal storage energy and exergy performance evaluations. *Renewable and Sustainable Energy Reviews*, 53:897–923, 2016. doi: 10.1016/j.rser.2015.09.006.

[2] M. Ryms and E. Klugmann-Radziemska. Possibilities and benefits of a new method of modifying conventional building materials with phase-change materials (PCMs). *Construction and Building Materials*, 211:1013–1024, 2019. doi: 10.1016/j.conbuildmat.2019.03.277.

[3] M. Javidan, M. Asgari, M. Gholinia, M. Nozari, A. Asgari, and D.D. Ganji. Investigation of convection and radiation heat transfer of paraffinic materials and storage of thermal energy in melting process of PCMs in the cavity with transparent inner walls. *Energy Reports*, 8:5522–5532, 2022. doi: 10.1016/j.egyr.2022.04.025.

[4] J. Guo, Z. Liu, Z. Du, J. Yu, X. Yang, and J. Yan. Effect of fin-metal foam structure on thermal energy storage: An experimental study. *Renewable Energy*, 172:57–70, 2021. doi: .10.1016/j.renene.2021.03.018

[5] J. Majeed, J. Abdulateef, and M. Zych. Thermal performance enhancement of triplex tube heat storage using metal foam. *Diyala Journal of Engineering Sciences*, 15(4):62–71, 2022. doi: 10.24237/djes.2022.15406.

[6] S. Al Arni, H.S. Sultan Aljibori, A.M. Abed, H.I. Mohammed, J.M. Mahdi, H. Togun, A.M. Sadeq, M. Ghalambaz, and N. Ben Khedher. Accelerated discharging kinetics in zigzag-shaped triplex-tube latent heat storage with nano-modified phase change materials additives. *Case Studies in Thermal Engineering*, 70:106140, 2025. doi: 10.1016/j.csite.2025.106140.

[7] F.L. Rashid, M. Eisapour, R.K. Ibrahem, P. Talebizadehsardari, K. Hosseinzadeh, M.H. Abbas, H.I. Mohammed, A. Yvaz, and Z. Chen. Solidification enhancement of phase change materials using fins and nanoparticles in a triplex-tube thermal energy storage unit: Recent advances and development. *International Communications in Heat and Mass Transfer*, 147:106922, 2023. doi: 10.1016/j.icheatmasstransfer.2023.106922.

[8] A.A. Al-Abidi, S. Mat, K. Sopian, M.Y. Sulaiman, and A.T. Mohammad. Internal and external fin heat transfer enhancement technique for latent heat thermal energy storage in triplex tube heat exchangers. *Applied Thermal Engineering*, 53(1):147–156, 2013. doi: 10.1016/j.applthermaleng.2013.01.011.

[9] S. Mat, A.A. Al-Abidi, K. Sopian, M.Y. Sulaiman, and A.T. Mohammad. Enhance heat transfer for PCM melting in triplex tube with internal-external fins. *Energy Conversion and Management*. 74:223–236, 2013. doi: 10.1016/j.enconman.2013.05.003.

[10] A.A. Al-Abidi, S. Mat, K. Sopian, M.Y. Sulaiman, and A.T. Mohammad. Experimental study of melting and solidification of PCM in a triplex tube heat exchanger with fins. *Energy and Buildings*, 68:33–41, 2014. doi: 10.1016/j.enbuild.2013.09.007.

[11] A. Yawar, J. Mohammadpour, A. Fattahi, and F. Salehi. A computational analysis for maximizing efficiency in triplex tube latent thermal energy storage. *Energy and Built Environment*, 2025. doi: 10.1016/j.enbenv.2025.05.011.

[12] P. Yan, W. Fan, Y. Yang, H. Ding, A. Arshad, and C. Wen. Performance enhancement of phase change materials in triplex-tube latent heat energy storage system using novel fin configurations. *Applied Energy*, 327:120064, 2022. doi: 10.1016/j.apenergy.2022.120064.

[13] M. Alizadeh, Kh. Hosseinzadeh, M.H. Shahavi, and D.D. Ganji. Solidification acceleration in a triplex-tube latent heat thermal energy storage system using V-shaped fin and nano-enhanced phase change material. *Applied Thermal Engineering*, 163:114436, 2019. doi: 10.1016/j.applthermaleng.2019.114436.

[14] C.C. Chueh and S.C. Hung. Numerical investigation of melting of a phase-change material in H-type shell tubes. *Applied Thermal Engineering*, 236:121470, 2024. doi: 10.1016/j.applthermaleng.2023.121470.

[15] B. Palmer, A. Arshad, Y. Yang, and C. Wen. Energy storage performance improvement of phase change materials-based triplex-tube heat exchanger (TTHX) using liquid-solid interface-informed fin configurations. *Applied Energy*, 333:120576, 2023. doi: 10.1016/j.apenergy.2022.120576.

[16] H. Waqas, M. Hussain, S. Khalid, Q.M. Al-Mdallal, and T. Muhammad. Investigation of the impact of triangular shape fins to enhancing the melting rate of phase change materials in triplex tube heat exchanger. *International Communications in Heat and Mass Transfer*, 162:108601, 2025. doi: 10.1016/j.icheatmasstransfer.2025.108601.

[17] A. Kumar, A. Maurya, M.I.H. Siddiqui, I.A. Alnaser, and I. Ashraf. Transient analysis of PCM discharging in a rotary triplex tube with wave-shaped fins. *Journal of Energy Storage*, 79:110178, 2024. doi: 10.1016/j.est.2023.110178.

[18] Z. Esmaeili, S.M. Vahidhosseini, S. Rashidi, and R. Rafee. Latent heat thermal energy storage enhancement in triplex tube heat exchangers: A comparative study on different tree-shaped fin structures. *International Communications in Heat and Mass Transfer*, 157:107794, 2024. doi: 10.1016/j.icheatmasstransfer.2024.107794.

[19] M. Boujelbene, J.M. Mahdi, A.M. Abed, M.S. Ghanim, K.A. Hammoodi, H.I. Mohammed, H. Togun, and P. Talebizadehsardari. The potential of arch-shaped fins for energy-charge enhancement in triplex-tube heat storage: Comparative analysis and optimization. *Journal of Energy Storage*, 79:110188, 2024. doi: 10.1016/j.est.2023.110188.

[20] F. Ren, J. Du, Y. Cai, J. Gou, Y. Liu, D. Zhang, and M. Li. Study on thermal performance of a new optimized snowflake longitudinal fin in vertical latent heat storage. *Journal of Energy Storage*, 50:104165, 2022. doi: 10.1016/j.est.2022.104165.

[21] M.M. Farid, A.M. Khudhair, S.A.K. Razack, and S. Al-Hallaj. A review on phase change energy storage: materials and applications. *Energy Conversion and Management*, 45(9-10):1597–1615, 2004. doi: 10.1016/j.enconman.2003.09.015.

[22] H. Xu, N. Wang, C. Zhang, Z. Qu, and M. Cao. Optimization on the melting performance of triplex-layer PCMs in a horizontal finned shell and tube thermal energy storage unit. *Applied Thermal Engineering*, 176:115409, 2020. doi: 10.1016/j.applthermaleng.2020.115409.

[23] V.V. Tyagi and D. Buddhi. PCM thermal storage in buildings: A state of art. *Renewable and Sustainable Energy Reviews*, 11(6):1146–1166, 2007. doi: 10.1016/j.rser.2005.10.002.

[24] H. Mehling, M. Brütting, and T. Haussmann. PCM products and their fields of application – An overview of the state in 2020/2021. *Journal of Energy Storage*, 51:104354, 2022. doi: 10.1016/j.est.2022.104354.
[25] G. Liu, Q. Li, J. Wu, R. Xie, Y. Zou, A. Marson, A. Scipioni, and A. Manzardo. Improving system performance of the refrigeration unit using phase change material (PCM) for transport refrigerated vehicles: An experimental investigation in South China. *Journal of Energy Storage*, 51:104435, 2022. doi: 10.1016/j.est.2022.104435.
[26] J. Zhang, Z. Cao, S. Huang, X. Huang, Y. Han, C. Wen, J.H. Walther, and Y. Yang. Solidification performance improvement of phase change materials for latent heat thermal energy storage using novel branch-structured fins and nanoparticles. *Applied Energy*, 342:121158, 2023. doi: 10.1016/j.apenergy.2023.121158.
[27] S. Entezari, A. Taheri, M. Khatibi, and H. Niazmand. Acceleration of melting process of phase change material using an innovative triplex-tube helical-coil storage unit: Three-dimensional numerical study. *Journal of Energy Storage*, 39:102603, 2021. doi: 10.1016/j.est.2021.102603.
[28] B. Çiçek. A numerical comparison of the thermal performances of nano-PCM heat sinks with Fe3O4, MgO, ZnO and xGNP nanoparticles: Key role of increased thermal conductivity. *Thermal Science and Engineering Progress*, 63:103712, 2025. doi: 10.1016/j.tsep.2025.103712.
[29] P. Saini, A. Dhar, and S. Powar. Parametric optimization of a cesaro fins employed latent heat storage system for melting performance enhancement. *Journal of Energy Storage*, 51:104534, 2022. doi: 10.1016/j.est.2022.104534.
[30] S. Al Arni, H.S. Sultan Aljibori, A.M. Abed, H.I. Mohammed, J.M. Mahdi, H. Togun, A.M. Sadeq, M. Ghalambaz, and N. Ben Khedher. Accelerated discharging kinetics in zigzag-shaped triplex-tube latent heat storage with nano-modified phase change materials additives. *Case Studies in Thermal Engineering*, 70:106140, 2025. doi: 10.1016/j.csite.2025.106140.
[31] M. Najafin, A. Tavakoli, A. Wadi Al-Fatlawi, M. Yousefi, M. Mohammadi, A. Shahraki, and A. Kianifar. Accelerating melting time in a triplex tube heat exchanger thermal energy storage unit with micro-channels. *Journal of Energy Storage*, 77:109967, 2024. doi: 10.1016/j.est.2023.109967.
[32] A.R. Darzi, M. Farhadi, and K. Sedighi. Numerical study of melting inside concentric and eccentric horizontal annulus. *Applied Mathematical Modelling*, 36(9):4080–4086, 2012. doi: 10.1016/j.apm.2011.11.033.
[33] A.D. Brent, V.R. Voller, and K.J. Reid. Enthalpy-porosity technique for melting convection-diffusion phase change: application to the melting of a pure metal. *Numerical Heat Transfer*, 13(3): 297–318, 1988. doi:10.1080/10407788808913615.
[34] W.B. Ye, D.S. Zhu, and N. Wang. Numerical simulation on phase-change thermal storage/release in a plate-fin unit. *Applied Thermal Engineering*, 31(17-18):3871–3884, 2011. doi: 10.1016/j.applthermaleng.2011.07.035.
[35] A. NematpourKeshteli, M. Iasiello, G. Langella, and N. Bianco. Enhancing PCMs thermal conductivity: A comparison among porous metal foams, nanoparticles and finned surfaces in triplex tube heat exchangers. *Applied Thermal Engineering*, 7212:118623, 2022. doi: 10.1016/j.applthermaleng.2022.118623.
[36] R.L. Hamilton, and O. K. Crosser. Thermal Conductivity of Heterogeneous Two-Component Systems. *Industrial and Engineering Chemistry Fundamentals*, 1(3):187--191, 1962. doi: 10.1021/i160003a005.
[37] K. Khanafer and K. Vafai. A review on the applications of nanofluids in solar energy field. *Renewable Energy*, 123:398–406, 2018. doi: 10.1016/j.renene.2018.01.097.